Construction and Building Materials 185 (2018) 310–324

Contents lists available at ScienceDirect

Construction and Building Materials

journal homepage: www.elsevier.com/locate/conbuildmat

Improving the shear performance of reinforced concrete beams made of recycled coarse aggregate

Emad E. Etman, Hamdy M. Afefy *, Ahmed T. Baraghith, Sara A. Khedr

Structural Engineering Dept., Faculty of Engineering, Tanta University, Tanta, Egypt

HIGHLIGHTS

- The shear capacity of RC made of recycled coarse aggregate was studied experimentally.
- The effect of the replacement ratio of the recycled aggregate has been investigated.
- Compensating the lost capacity was restored by providing internal short fibers.
- Curing the recycled aggregate enabled the RC beams made of recycled aggregate to be enhanced.

ARTICLE INFO

Article history:
Received 12 April 2018
Received in revised form 9 July 2018
Accepted 11 July 2018
Available online 18 July 2018

Keywords:
Recycled coarse aggregate
Shear strength
Curing methods
Polypropylene fiber
Shear design
Codes and standard

ABSTRACT

This paper investigates experimentally and analytically the shear performance of RC beams made of recycled coarse aggregate (RCA). Previous studies showed that the partial replacement of the virgin coarse aggregate by recycled one results in decrease the shear strength of RC beams. Consequently, the main target of the this research was to compensate such decrease in the shear strength by providing internal short fibers and using cured recycled coarse aggregate instead of crude recycled coarse aggregate. A total of eleven simply supported RC beams made of recycled coarse aggregate along with one conventional concrete beam were tested under incremental four-point loading scheme. The considered parameters were the recycled coarse aggregate replacement ratio (15, 30 and 45%), the shear span-to-depth ratio (1, 2 and 3) and the fiber volumetric ratio (1, 1.5 and 2%). In addition, to improve the physical and mechanical properties of the recycled coarse aggregate (RCA), two curing methods for the RCA were implemented using cement slurry and Styrene Butadiene Rubber (SBR) compound. The experimental results showed that increasing the replacement ratio of the RCA resulted in decrease the shear capacity proportionally. The percentages of decreases in the shear capacities were about 8%, 14% and 19%, respectively, for RC beams provided by RCA replaced by 15%, 30% and 45%. In addition, it was shown that providing internal short fibers by volumetric ratios of 1%, 1.5% and 2% enabled the RC beams made of 30% partial replacement of the recycled coarse aggregate to compensate the decreases in the shear capacities (14%) and to increase their shear capacities by about 13%, 15% and 22% compared to those of the control beam, respectively. Furthermore, for RC beams made of 30% partial replacement of the RCA, the shear capacities decreased by about 2%, 14% and 37%, respectively, for beams having shear span-to-depth ratio of 1, 2 and 3. Besides, it was shown that, the cured recycled coarse aggregate enabled the RC beams made of 30% partial replacement to exhibit improved shear performance. However, the curing method based on cement slurry showed higher improvement since the restored shear capacities were about 15% and 3% for beams provided by cured coarse aggregate based on cement slurry and compound SBR, respectively compared to that of the beam made of crude RCA. Finally, an equation for estimating the shear capacity of RC beams made of recycled coarse aggregate was proposed and it showed satisfactory results when verified against the experimental findings of the current research as well as of other researches where the maximum variations were about 8.5% and 22%, respectively.

© 2018 Elsevier Ltd. All rights reserved.

1. Introduction

Currently, the amount of demolition wastes resulting from concrete buildings due to the expired life time of the buildings and/or

* Corresponding author at: Structural Engineering Dept., Faculty of Engineering, Tanta University, Tanta 31511, Egypt.
E-mail address: hamdy.afefy@f-eng.tanta.edu.eg (H.M. Afefy).

https://doi.org/10.1016/j.conbuildmat.2018.07.065
0950-0618/© 2018 Elsevier Ltd. All rights reserved.

the terrorism attack and recent wars are becoming an environmental problem. Thus, recycling of concrete waste represents a new way to get rid of such demolition waste as well as to find out a new resource for the concrete production. It is well recognized that the main component of the concrete is the coarse aggregate, which represents about 60% to 75% of concrete volume. Coarse aggregate is mainly obtained by blasting rock blocks and then by crushing them to the required size. This process is detrimental for the environment where it destroys mountains, erodes the soils, and produces huge quantities of Carbon Dioxide. Thus, using of recycled aggregate has many benefits such as economic aspects, preserving the consumption of limited resources and decreasing the environmental pollution. Generally, recycled coarse aggregate produced by crushing, screening and removing the impurities from the demolition waste [1]. In contrast, the rate of consumption of natural aggregate is rapidly increasing due to the production and utilization of concrete. Recycled aggregate could treat this problem by converting the waste product to a new resource for the coarse aggregate.

Cement paste and some amount of mortar from the original concrete remain attached to stone particles of recycled coarse aggregate. Consequently, the recycled coarse aggregate has lower density, higher porosity, and higher water absorption capability than those of the natural aggregate. Therefore, it is very essential to use the suitable curing or treatment techniques in order to maintain the moisture and temperature condition for the surface of the recycled coarse aggregate. Hydration using calcium aluminate hydrates or calcium silicate hydrate also known as cement gel is one type of recycled aggregate curing. Hydration reactions are continued until all the cement reaches its maximum degree of hydration or until the cement gel fills all the available space, whichever limit is reached first. As the hydration reactions proceed, the water-filled space in cement paste is increasingly replaced with solid hydration product, which results in increasing its strength and decreasing its permeability. Due to its nanoscale pore system and high water content, the calcium silicate hydrate gel is the primary phase affected by drying of cement paste. Thus, calcium silicate hydrate compound affect concrete hardening, while calcium aluminate hydrates compounds control the workability [2].

Water curing and steam curing [3] are other curing methods. Katz [4] treated the recycled aggregate by impregnation of the recycled coarse aggregate in silica fume solution and cleaning the recycled aggregate by ultrasonic. Results showed that impregnation of recycled aggregate in silica fume led to an increase of about 15 to 30% in the concrete compression strength at ages 7 to 28 days.

Some researchers investigated the use of chemical components to treat the recycled aggregate such as calcium metasilicate (CM), Nano silicate (NS), and HCL acid [5–7]. It was found that the RCA impregnated in calcium metasilicate (CM) solution resulted in better concrete strength than the RCA treated by Nano silicate (NS) In addition; the recommended optimum concentration of CM solution for treated coarse RCA was about 10% [5]. In addition, the surface treatment by presoaking the RCA in HCL acid at 0.1 M concentration effectively removed the loose mortar particles and thereby significantly improved the properties of the RCA [6]. Furthermore, the results showed that the behavior of RCA had improved with reduction in water absorption, without simultaneous exceeding the limits of chloride and sulphate compositions after the pre-soaking treatment approaches based on HCl, H_2SO_4 and H_3PO_4 [7].

Other researchers studied coating the recycled aggregate by cementitious and powder components such as cement slurry, Stone Envelope Pozzolanic Powder (SEPP), and Polyvinyl alcohol powder (PVA) [8,9]. It was found that the slump and strength results indicated that the new mixing technique of RCA based on stone enveloped with pozzolanic powder (SEPP) contributed significantly to better workability and higher compressive and flexural strengths. In addition, the interfacial transition zone was noticed to be denser than those patches prepared by normal mixing approach (NMA) or stone enveloped with Portland cement (SEPC) approach [8]. Furthermore, the test results showed that there was not only an improvement in the mechanical properties of the concrete made with PVA impregnated RCA, but also the shrinkage was noticed to be decreased [9].

The shear force in reinforced concrete beams is transferred through the concrete compression zone, the dowel action of flexural reinforcement, the aggregate interlock between the aggregate particles, and the transverse shear reinforcement. Whereas, the aggregate interlock defined as the interface transfer of shear force between the rough concrete crack faces. The efficiency of shear transfer through aggregate interlock is reduced if the coarse aggregate fractures at cracks [10]. Thus, the use of recycled coarse aggregate in structural RC member could lead to an adverse effect on the shear strength. As a consequent, many researchers devoted their effort to study the shear behavior of recycled aggregate RC beams. Whereas, they focused on the following parameters: recycled aggregate replacement ratio RCA% [11–22], longitudinal reinforcement ratio ρ%[11,21,23-25], shear span-to-depth ratio a/d [14,16-24,26,27] size effect [13,17,25,26], the amount of shear reinforcement [16,18,19,25], concrete compressive strength [20,22] and treatment method [25,26].

The majority of experimental test results conducted on the shear behavior of RC beams made of recycled coarse aggregate reach the same findings that could be summarized as follows:

- The shear strength declines with increasing the recycled aggregate replacement ratio [11-22].
- The shear strength decreases as the shear span-to-depth ratio increased while other parameters are held constant [14,16–24,26,27].
- Using treated recycled coarse aggregate increased the compressive and shear strengths compared to concrete made of untreated recycled aggregate [3–9,25,26].
- The crack pattern of recycled aggregate concrete beams and failure mode are alike to those of conventional concrete beams [11-14,22].
- Cracks widths of recycled aggregate concrete beams are wider than those of control beam due to weak aggregate interlock of recycled aggregate [8,20,21].
- Both conventional concrete and recycled aggregate concrete beams that provided with large percentage of transverse reinforcement do not produce any diagonal tension cracks [16,18,19,25].
- The evolution of shear cracks is severe in concrete with higher recycled aggregate replacement ratio and less longitudinal reinforcement ratio [11,21,23–25].
- The shear strength of recycled aggregate concrete beams decreased with increasing the effective depth regardless of replacement ratio [13,17,25,26].

In the current study, the shear performance of RC beams made of recycled coarse aggregate provided by 15%, 30% and 45% replacement ratio of the virgin coarse aggregate has been studied experimentally. Besides, in order to improve the aggregate interlock between the recycled coarse aggregate, polypropylene short fibers were provided with different volumetric ratios; namely, 1%, 1.5% and 2%. Furthermore, two curing techniques based on cement slurry and Styrene Butadiene Rubber (SBR) compound were implemented in order to enhance both physical and mechanical properties of the used recycled coarse aggregate.

2. Experimental program

2.1. Test specimens

The experimental program consisted of twelve reinforced concrete beams divided into 5 groups as summarized in Table 1. Four parameters had been investigated, namely; recycled coarse aggregate replacement ratio (15, 30 and 45%), shear span-to-depth ratio (1, 2 and 3), fiber volumetric ratio (1, 1.5 and 2%), and curing method of the recycled coarse aggregate (Cement slurry and SBR compound). All test specimens had the same concrete dimensions as well as the longitudinal steel reinforcements. The cross-section of the beams was rectangular section having 150 mm width and 300 mm total depth. The total span of all beams was 2000 mm, while the center-to-center span was 1800 mm. The test specimens were proportionated to fail in shear while the flexural capacity was probably guarded. The main steel of all beams were four deformed steel bars of 16 mm diameter, while the secondary steel contained two deformed steel bars of 16 mm diameter. The stirrups were made of smooth steel bars of 8 mm diameter, spaced every 100 mm and arranged according to shear span-to-depth ratio as depicted in Fig. 1. The shear span at the left side for all test beams was unreinforced to eliminate the effect of the vertical stirrups from the shear resistance of all beams.

2.2. Material properties

The used recycled coarse aggregate in the current research was produced by crushing old concrete cubes. After crushing the old concrete cubes, the sieve analysis was performed to collect the recycled coarse aggregate passing from sieve No. ¾″ of the opening size of 19 mm as depicted in Fig. 2. That is to have blended aggregate for different replacement ratio of the same maximum aggregate size. It can be observed that the recycled coarse aggregate was poorly graded in comparison with the natural coarse aggregate. That is because the quantities of the finer fractions increased with increasing the RCA replacement ratio owing to small particles resulted from the crushing process. In addition, the quantities of the coarser fractions also increased with increasing the RCA replacement ratio as a result of the adhered mortar to the RCA.

Ten concrete mixes have been prepared for the studied parameters as listed in Table 2, which design according to British Standard BS EN 206-1 [28] to have a concrete cube strength of about 30 MPa. The mixtures were proportioned with Portland cement type I with cement content of 350 kg per cubic meter, while the water-to-cement ratio was constant (W/C = 0.5). Four mixes were produced with different replacement ratio of recycled coarse aggregate (0, 15, 30, and 45%). Polypropylene fibers were added to another three mixes with volumetric ratios of the cement content as 1, 1.5, and 2%, while the coarse aggregate replacement ratio was kept 30%. For the remaining three mixes, recycled coarse aggregate was cured by cement slurry and SBR compound (Refer to Table 3). Typical polypropylene fibers (Fiber mesh 300) [29] of specific gravity of 0.91 and single-cut lengths have been chosen and used in the current study.

Different tests have been performed in order to obtain the physical properties of the used RCA such as specific gravity, bulk density, absorption ratio and the porosity as listed in Tables 4 to 7. It can be observed that increasing the RCA replacement ratio resulted in decrease both the specific density and the bulk density as well as increase the water absorption and the porosity ratios of the RCA

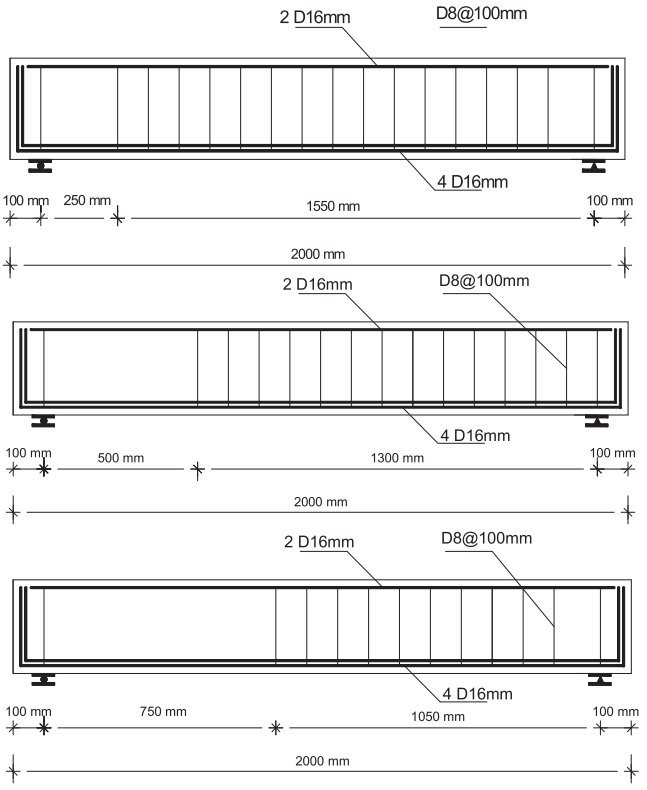


Fig. 1. Concrete dimensions and reinforcement detailing for all specimens.

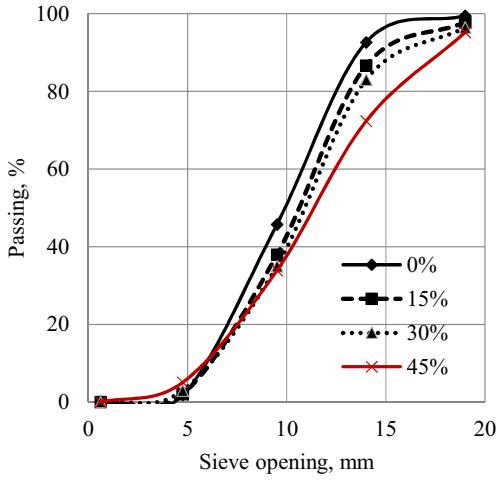


Fig. 2. Grading of natural and recycled coarse aggregate for different replacement ratios.

Table 1
Test matrix.

Group No.	Specimen	RCA %	a/d	V_f %	Curing method
G1	BI-2-0-0	0%	2	0%	NA
G2	BII-2-15-0	15%	2	0%	NA
	BII-2-30-0	30%	2	0%	NA
	BII-2-45-0	45%	2	0%	NA
G3	BIII-1-30-0	30%	1	0%	NA
	BIII-3-30-0	30%	3	0%	NA
G4	BIV-2-30-1	30%	2	1%	NA
	BIV-2-30-1.5	30%	2	1.5%	NA
	BIV-2-30-2	30%	2	2%	NA
G5	BV-2-30-0-C1	30%	2	0%	Cement Slurry
	BV-2-30-0-C2	30%	2	0%	Compound SBR
	BV-2-30-1.5-C1	30%	2	1.5%	Cement Slurry

RCA = recycled aggregate replacement ratio; a/d = shear span-to-depth ratio; V_f = polypropylene fiber volumetric ratio; NA = not applicable.

Table 2
Concrete mixes and mechanical properties for the hardened test specimens.

Mix No.	RCA (%)	V_f (%)	Curing method	Mix proportions (kg/m^3)					f_{cu} MPa	f_t MPa	f_r MPa
				W/C	Cement	Sand	Coarse aggregate				
							Recycled	Natural			
Mix (1)	0%	0	——	0.5	350	535	0	1279	28.80	2.30	4.60
Mix (2)	15%	0	——	0.5	350	535	192	1087	28.20	2.25	4.51
Mix (3)	30%	0	——	0.5	350	535	384	895	26.90	2.15	4.30
Mix (4)	45%	0	——	0.5	350	535	576	703	25.00	1.87	4.00
Mix (5)	30%	1%	——	0.5	350	535	384	895	28.31	2.28	4.51
Mix (6)	30%	1.5%	——	0.5	350	535	384	895	29.30	2.31	4.68
Mix (7)	30%	2%	——	0.5	350	535	384	895	31.90	2.39	5.10
Mix (8)	30%	0	Cement slurry	0.5	350	535	384	895	29.75	2.23	4.76
Mix (9)	30%	0	Compound SBR	0.5	350	535	384	895	27.50	2.20	4.41
Mix (10)	30%	1.5	Cement slurry	0.5	350	535	384	895	30.90	2.32	4.94
Average									28.66	2.23	4.58
Standard deviation									1.98	0.14	0.32
Coefficient of variation (COV)									0.07	0.06	0.07

RCA = recycled aggregate replacement ratio; V_f = polypropylene fiber volumetric ratio; f_{cu} = concrete compressive cube strength; f_t = split cylinder tensile strength; f_r = modulus of rupture strength.

Table 3
Technical data of Styrene Butadiene Rubber (SBR).

Specific gravity @ 25 °C	pH	Total solids	Full cure time @ 25 °C
1.01	9.5	47%	48 h @ 1.3 mm thickness

Table 4
Apparent density (Specific gravity) (SSD) for the used recycled coarse aggregate.

Sample No.	RCA%	Curing method	Weight of sample, gm.		SSD
			NA	RA	
1	0	No curing	400	0	2.70
2	15	No curing	340	60	2.58
3	30	No curing	280	120	2.50
4	45	No curing	220	180	2.43
5	30	Cement slurry	280	120	2.60
6	30	Compound SBR	280	120	2.54

NA = Natural Aggregate; RA = Recycled aggregate; RCA% = recycled aggregate replacement ratio; SSD = specific gravity.

Table 5
Bulk density (OD) for the used recycled coarse aggregate.

Sample No.	RCA%	Curing method	W, gm.	V, cm^3	OD, gm/cm^3
1	0	No curing	9475	2200π	1.371
2	15	No curing	9376	2200π	1.356
3	30	No curing	9023	2200π	1.305
4	45	No curing	8828	2200π	1.277
5	30	Cement slurry	9125	2200π	1.320
6	30	Compound SBR	9108	2200π	1.317

OD = Bulk density; W = weight of proportional (recycled and natural) in mold; V = volume of mold.

Table 6
Absorption, % for the used recycled coarse aggregate.

Sample No.	RCA%	Curing method	m_1, gm.	m_2, gm.	A %
1	0	No curing	2037	2006	1.98
2	15	No curing	2026	1975	2.58
3	30	No curing	2043	1967	3.863
4	45	No curing	2023	1944	4.06
5	30	Cement slurry	2034	1977	2.88
6	30	Compound SBR	2016	1964	2.46

m_1 = Wetted weight of aggregate in gm; m_2 = Dried weight of aggregate in gm; A % = Absorption ratio.

Table 7
Porosity, % for the used recycled coarse aggregate.

Sample No.	RCA%	Curing method	Porosity, %
1	0	No curing	0.209
2	15	No curing	0.329
3	30	No curing	0.475
4	45	No curing	0.479
5	30	Cement slurry	0.370
6	30	Compound SBR	0.330

compared to those of natural coarse aggregate. However, curing the RCA enabled it to show some enhancement in the physical properties of the recycled coarse aggregate keeping the same RCA replacement ratio.

Three typical standard concrete cubes of 150 × 150 × 150 mm were cast for each concrete patch to obtain the concrete compressive strength. Moreover, three standard concrete cylinders of 150 mm diameter by 300 mm total height were cast for each patch in order to obtain splitting tensile strength. Furthermore, standard prisms of square cross-section of 150 mm side length and 600 mm long were cast to carry out the modulus of rupture test. The standard cubes, cylinders and prisms were prepared and stored in moist room, then tested after 28 days. The average concrete compressive strength, the concrete tensile strength and the modulus of rupture strength for hardened concrete are summarizes in Table 2.

Deformed steel bars of 420 MPa yield strength were used for both tensile and compressive longitudinal reinforcement while smooth bars of 270 MPa yield strength were used for vertical stirrups

2.3. Preparing and curing of recycled aggregate

During the production process of the recycled coarse aggregate, an amount of old cement paste remains attached to the recycled aggregate that responsible for lower density, higher porosity, and higher water absorption than those of virgin aggregate. Thus, it is important to remove the attached mortar to improve the quality of the recycled coarse aggregate. That can be done by increasing the cycles of treatment processes employed in recycling plants. Nonetheless, by product large amount of powder was produced. Hence, special capability is needed for effective production of high quality recycled coarse aggregate. Alternatively, suitable curing methods are used in order to keep the design mixing water. In the current study, two curing method have been proposed to

improve both physical and mechanical properties of the used recycled coarse aggregate.

2.3.1. Coating by cement slurry

This technique had been used by Kukadia et al. [30] and Shrinath et al. [31]. Kukadia et al. [30] cured the recycled coarse aggregate by cement slurry where the cement was used by an amount of 10% by the weight of solution water. On the other hand, Shrinath et al. [31] prepared coating cement slurry in which the cement content was used by an amount of 67% by weight of solution water.

In the current study, the recycled aggregate in mixes no. (8 and 10) illustrated in Table 2 was coated by cement slurry while the recycled coarse aggregate replacement ratio was kept 30%. So, the cement content was 9.45 kg per 0.09 m^3 which equal 30% from cement content of 350 kg per 1 m^3. The recycled coarse aggregate was impregnated in cement slurry in mixer drum and mixed for about five minutes, then, it was spread on wooden blank as shown in Fig. 3(a). The cement slurry coated the recycled aggregate and filled the empty voids.

2.3.2. Curing by SBR compound.

Styrene Butadiene Rubber (SBR) is a polymer system consisted of very small particles (0.05 to 10μ m diameter) which could improve the bond between recycled aggregate. The dosage of compound SBR was in the form of polymer/cement ratios as 5%, 10% and 15% [32]. In the current study, the polymer/cement ratio of SBR compound was chosen as 10% with total solids ratio of 47%. The technical data of SBR compound is summarized in Table 3. The recycled aggregate immersed in compound SBR in mixer drum as depicted in Fig. 3(b) and mixed for about five minutes, then, it was spread on wooden blank till the cured coarse aggregate had been dried.

For both curing methods, the cured recycled coarse aggregate was exposed indoor to air drying for about 4 days where the ambient temperature was about 28 °C and the humidity was about 55% and then it used to produce the cured recycled aggregate patches (Mixes (8), (9) and (10) at Table 2) for group No. 5 as illustrated in Table 1.

2.4. Set up and instrumentation

The test specimens were tested under four point loading scheme with three different values of shear span-to-depth ratio (1, 2 and 3). The beams were simply supported as depicted in Fig. 4. At the un-reinforced shear span side, two Linear Variable Differential Transformers (LVDTs) of 100 mm measuring length were arranged at right angle in order to obtain the developed shear strain. Khaja and Sherwood [23] measured the shear strain on the faces of each specimens at the quarter-span by side-mounted linear variable differential transformers with the aid of Eq. (1).

$$\gamma = \frac{\delta_2 - \delta_1}{\sqrt{L_2^2 + L_1^2}} \quad (1)$$

Where γ is the shear strain; δ_2 is the LVDT's readings in the direction parallel to the developed shear cracks; δ_1 is the LVDT's readings in the perpendicular direction; L_1 and L_2 are the distances between the fixed points of the LVDTs in the perpendicular and parallel directions of the shear cracks ($L_1 = L_2 = 200$ mm).

Furthermore, one LVDT of 50 mm gauge length was used in order to measure the developed mid-span deflection as depicted in Fig. 4. The developed tensile normal strain on the main tensile steel bars was measured by 6 mm gauge length strain gauge, while two Pi-gauges of 100 mm gauge length were used to measure the developed deformations on the concrete surface at both tension and compression sides at the mid-span section. The beams were



(a) recycled aggregate cured by cement slurry (b) recycled aggregate cured by compound SBR

Fig. 3. Cured recycled coarse aggregate.



Fig. 4. Test set up.

loaded incrementally considering the load control scheme at two points through a loading steel beam. Consequently, the beam was loaded in several steps at a loading rate ranged from 0.1 to 0.2 kN/s up to complete failure. The acting load was measured by a load cell of 500 kN capacity. After each loading step, the vertical mid-span deflection, the LVDTs readings, the Pi-gauge readings, the developed normal strains in the longitudinal steel bars were recoded and stored using an automatic data logger unit (TDS-150).

3. Experimental results

The exhibited modes of failure, the cracking and ultimate loads, cracks characteristics, deflection behavior, and the developed shear strain on the concrete surface are selectively considered and compared for all test specimens. That is to highlight the differences in the shear behavior for recycled concrete beams owing to different replacement ratios of the coarse aggregate, different fiber volumetric ratios and different curing techniques.

3.1. Modes of failure and crack pattern

For all tested beams, at early loading stage, flexural cracks were first developed around the pure moment zone. With further loading, the flexural cracks were propagated at the tension side till the appearance of shear cracks at the unreinforced side. As the load increased, the diagonal shear cracks were widen and extended to reach the line connecting the supporting point and the loading point. In the meantime, shear cracks with narrower width were developed at the reinforced side until the shear failure occurred at the unreinforced side. It could be noticed that the crack pattern of recycled aggregate concrete beams and failure mode are similar to those of conventional concrete beams as depicted in Figs. 5 to 8 and as documented by other researches [12–14,19].

It could be observed that increasing the recycled aggregate replacement ratio as for beams of group G2 resulted in accelerating the appearance of both flexural and shear cracks as summarized in Table 4. While the recycled aggregate replacement ratio was kept constant as for the beams of group G3, the crack propagation depends on shear span-to-depth ratio. For beam BIII-3-30-0 with shear span-to-depth ratio equals to 3, cracks propagated suddenly with a little change of load. This failure mode is called "Diagonal Tension" failure. For beam BIII-1-30-0 with shear span-to-depth ratio equals to 1, the cracks propagated very gradually toward the point load. This failure mode is called "Compression" failure. For beam BII-2-30-0 with shear span-to-depth ratio equals to 2, the cracks propagated regularity with a transition stage between the former two cases. This failure mode is called "Shear Tension" failure.

Adding internal discrete fibers and curing by cement slurry resulted in an increase on both secant stiffness and ultimate load-carrying capacity. In addition, the manifested failure mode was more ductile than that of recycled aggregate concrete specimen without neither internal discrete fibers nor curing. Besides, the developed shear cracks for beams provided with polypropylene discrete fibers were narrower and more closely due to the bridging action of the internal fibers as depicted in Figs. 7 and 8.

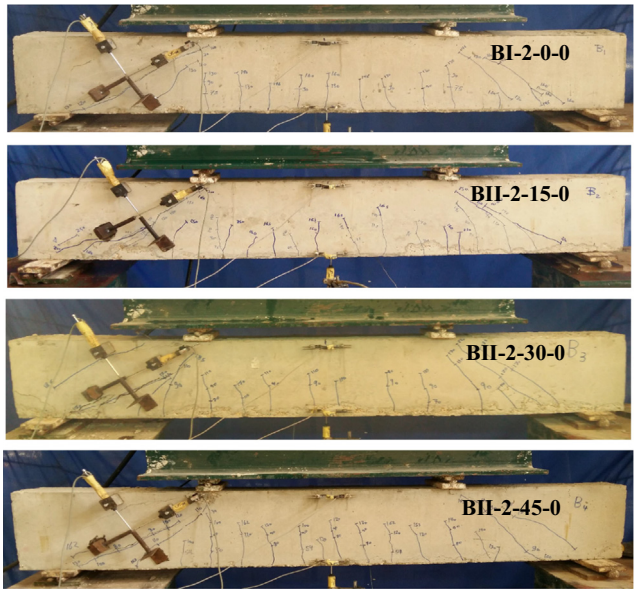


Fig. 5. Crack pattern for all test specimens of group G2.

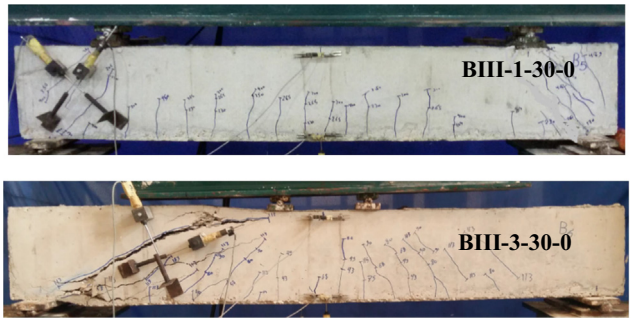


Fig. 6. Crack pattern for all test specimens of group G3.

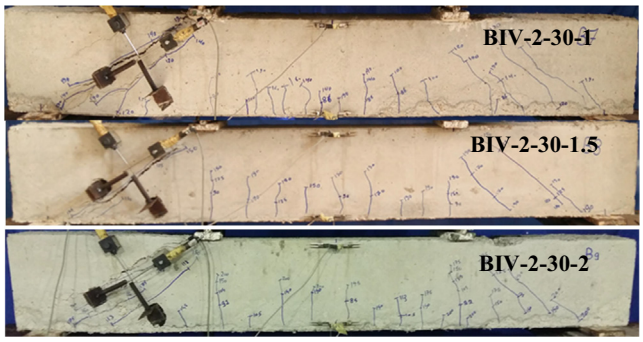


Fig. 7. Crack pattern for all test specimens of group G4.



Fig. 8. Crack pattern for all test specimens of group G5.

3.2. Cracking and ultimate loads

Table 8 summarizes the experimental values for the first flexural cracking load, the first shear cracking load, and the failure load for all test specimens. The experimental results for group G2 showed that the cracking and failure loads of specimens decreased by increasing the recycled coarse aggregate replacement ratio as expected. For the recycled coarse aggregate replacement ratios 15, 30 and 45%, the decreases in the failure loads are 8, 14 and 19% respectively, compared to that of the control beam BI-2-0-0.

In addition, increasing the shear span-to-depth ratios as implemented in group G3, while keeping the recycled aggregate replacement ratio to 30% resulted in decrease the shear capacity proportionally. The shear capacities are 175, 153, and 113 kN for beams having shear span-to depth ratios of 1, 2 and 3%, respectively. On contrary, adding polypropylene discrete fibers to the recycled aggregate mixtures led to increase the shear capacity. That is because of the provided fibers enhanced the aggregate interlock between recycled aggregate. The percentage of increases in the failure load for tested beams in group G4 with fiber volumetric ratios of 1, 1.5 and 2% are 32, 34 and 41%, respectively, compared to that of beam BII-2-30-0.

The curing methods by cement slurry and compound SBR improved the mechanical and physical properties of the recycled aggregate since the ultimate shear capacities of all specimens of group G5 had increased compared to that of the beam incorporated uncured recycled aggregate. The failure load for tested beams with cement slurry and compound SBR curing method increased by about 15% and 3%, respectively compared to that of beam BII-2-30-0. Moreover, the failure load of the cured beam BV-2-30-1.5-C1 provided with fiber volumetric ratio of 1.5% increased by 8% compared to that of the beam BIV-2-30-1.5 without curing.

3.3. Cracks characteristics

For all specimens, the major shear crack widths at different loading levels were measured and traced against the jacking load as depicted in Figs. 9 and 10. In addition, the number of developed shear cracks at the final loading stage was counted and listed in Table 8.

It can be observed that increasing the coarse aggregate replacement ratio (group G2) led to increase the major crack width at the same loading level as depicted in Fig. 9(a). Although the ultimate capacities decreased by about 8%, 14% and 19% for replacement ratios of 15, 30 and 45%, respectively, the final crack widths showed increases by 27, 39 and 96%, respectively, compared to that of the control specimen BI-2-0-0. In addition, since the recycled aggregate is weaker than the natural virgin one, the number of developed cracks increased by increasing the replacement ratio as listed in Table 8.

As for the shear span-to-depth ratio (group G3), the major shear crack width increased as the shear span-to-depth ratio increased at the same loading level (refer to Fig. 9(b)), while the number of shear cracks decreased as the shear span-to-depth ratio increased as listed in Table 8.

As depicted in Fig. 10(a), providing internal polypropylene discrete fibers by volumetric ratio of 1% enabled the beam BIV-2-30-1 to show narrower crack width than that of the beam BII-2-30-0 at

Table 8
Experimental measurements for all test beams.

Group No.	Specimen	$P_{cr,f}$, kN	$P_{cr,sh}$, kN	P_u, kN	δ_{max}, mm	Average stiffness kN/mm	Strain energy kN.mm	Wcr, mm	N	ε_{max}, $*10^{-6}$	γ $*10^{-6}$
G1	BI-2-0-0	75	120	178	5.10	34.5	791	1.523	2	1711	7530
G2	BII-2-15-0	69	111	164	6.37	26.1	866	1.93	2	1387	8912
	BII-2-30-0	55	73	153	7.40	21.1	755	2.12	3	1253	12,205
	BII-2-45-0	39	71	144	7.92	19.2	593	2.99	4	1152	19,510
G3	BIII-1-30-0	58	83	175	7.98	25.8	1055	0.92	4	1369	8080
	BIII-3-30-0	43	58	113	6.43	19.3	1095	2.22	2	1134	13,845
G4	BIV-2-30-1	72	95	202	7.12	27.7	1263	1.9	4	1769	11,914
	BIV-2-30-1.5	74	98	205	6.07	40.1	957	1.63	3	1802	9512
	BIV-2-30-2	79	104	217	5.65	42.2	1180	1.51	3	1977	8757
G5	BV-2-30-0-C1	69	86	176	6.74	26.1	681	1.55	3	1819	9457
	BV-2-30-0-C2	49	74	158	7.13	22.7	688	1.75	4	1269	10,084
	BV-2-30-1.5-C1	93	125	221	5.98	45.8	1088	1.17	2	1958	8162

$P_{cr,f}$ = first flexural cracking load; $P_{cr,sh}$ = first shear cracking load; P_u = failure load; δ_{max}= maximum mid-span deflection; Wcr = crack width for major shear crack at failure; N: = number of developed shear cracks on the concrete side; ε_{smax}= maximum developed tensile normal strain on the main tension steel; γ= maximum shear strain.

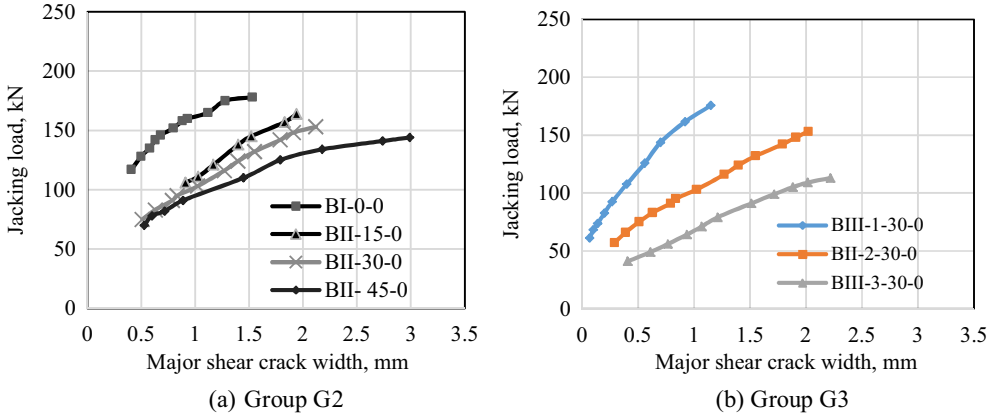


Fig. 9. Development of the major shear crack width for the tested specimens of groups G2 and G3.

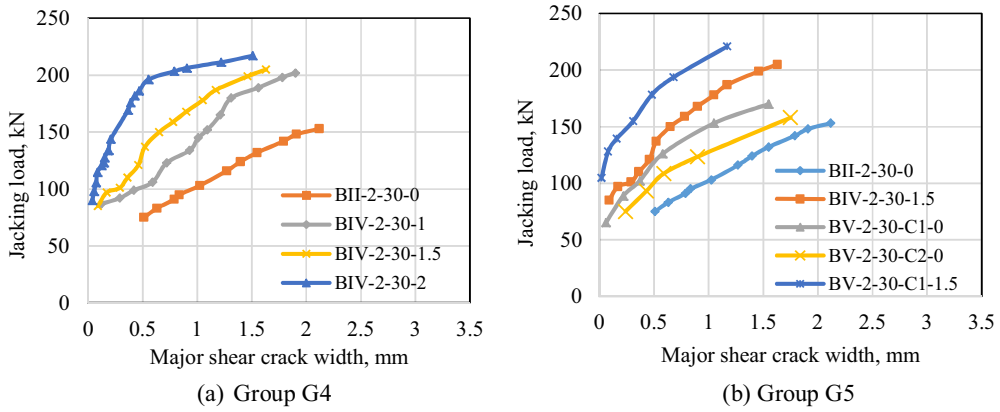


Fig. 10. Development of the major shear crack width for the tested specimens of groups G4 and G5.

the same loading level. However, the developed crack widths of beam BIV-2-30-1 still higher than that developed by control beam BI-2-0-0. Increasing the fiber volumetric ratio further to 1.5 and 2% enabled the beams BIV-2-30-1.5 and BIV-2-30-2 to show narrower cracks widths than that of the control beam BI-2-0-0 owing to the increased bridging effect of the internal fibers.

Curing the recycled coarse aggregate resulted in decrease the exhibited major shear crack width. That could be attributed to the enhanced mechanical properties of the cured coarse aggregate where the aggregate interlock had been improved. For group G5, the major shear crack width of beams BV-2-30-0-C1 and BV-2-30-0-C2 cured with cement slurry and compound SBR decreased by about 27% and 17%, respectively, compared to that of beam BII-2-30-0. Besides, the major shear crack width of beam BV-2-30-1.5-C1decreased by about 28% compared to that of beam BIV-2-30-1.5 as listed in Table 8.

3.4. Deflection behavior

Table 8 lists the recoded maximum mid-span deflection,δ_{max}, for all beams in addition the entire deflection plateaus at different loading stages are depicted in Figs. 11 and 12. It is worth mentioning that after the occurrence of the shear failure, the jacking load was released gradually. That was done in order to trace any developed softening behavior.

It can be observed that the load-deflection curves for all test specimens were approximately linear up to near the failure load and then dropped linearly after failure. However, the test parameters affect the ultimate load-carrying capacity as well as the corresponding mid-span deflection for all beams. Thus, the average secant stiffness of the linearly load-deflection curve was calculated in addition to the exhibited strain energy by each beam (the area under the load-deflection curve) as summarized in Table 8.

It can noticed that increasing the recycled aggregate replacement ratio resulted in increase the exhibited mid-span deflection at the same loading level as depicted in Fig. 11(a). That can be attributed to the presence of minute pores in the adhered mortar to the RCA along with the developed continuous cracks and fissures inside the RCA due to the crushing process. Such effects resulted in increasing the weakness of the concrete accompanied by accelerating the appearance of both flexural and shear cracks as the RCA replacement ratio increased as illustrated in Table 8. Thus the stiffness decreased by about 25%, 39% and 44% for beams provided by 15%, 30% and 15% RCA replacement ratios, respectively, compared to that of the control beam without any RCA. However, the developed strain energies did not decrease by such value as illustrated in Table 8. That could be attributed to the increased mid-span deflection with increasing the RCA replacement ratio insipte the manifested declination in the ultimate load-carrying capacity.

Fig. 11(b) shows that increasing the shear span-to-depth ratio enabled the failed beam BIII-3-30-0 to exhibit some soften plateau owing to the flexural effect. Nevertheless, increasing the shear span-to-depth ratio resulted in increase the exhibited mid-span deflection as depicted in Fig. 11(b). Thus, the developed strain energy showed significant enhancement by about 33% and 38% for beams BIII-1-30-0 and BIII-3-30-0, respectively, compared to that of the control beam BI-0-0. However, the average secant

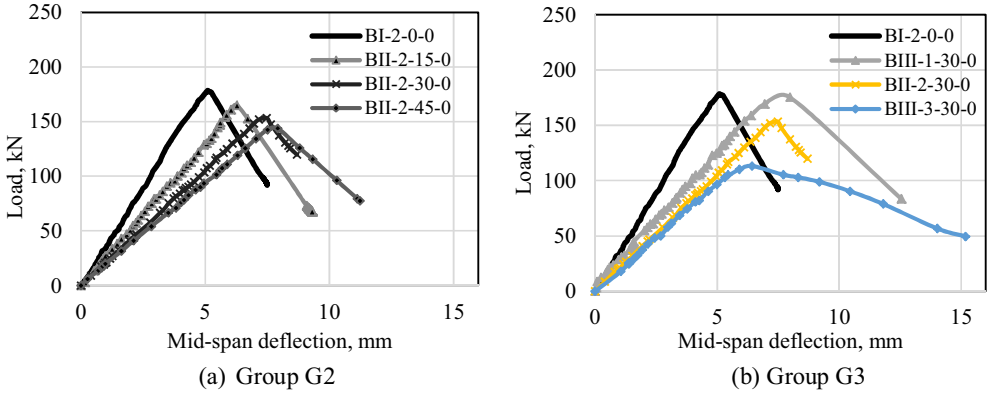


Fig. 11. Load versus mid-span deflection for all specimens of groups G2 and G3.

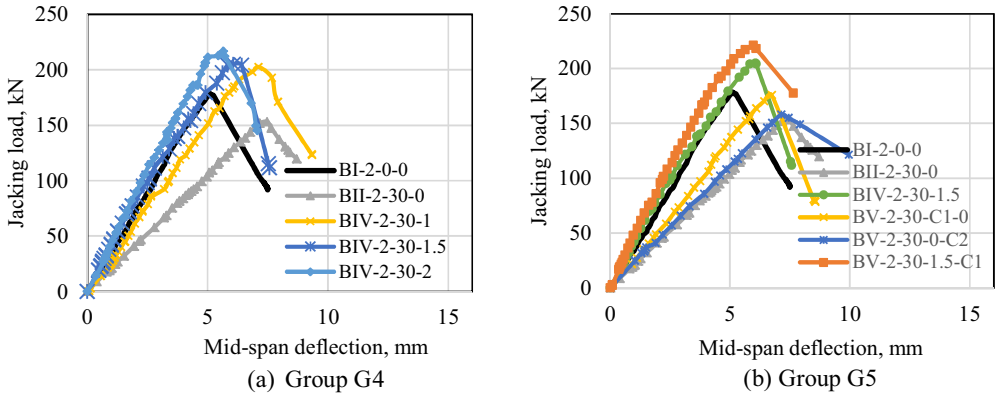


Fig. 12. Load versus mid-span deflection for all specimens of groups G4 and G5.

stiffness decreased by about 25% and 44% for beams BIII-1-30-0 and BIII-3-30-0, respectively, compared to that of the control beam BI-0-0. Although, the stiffness of beam BIII-1-30-0 showed significant increase by about 22% compared to that of BII-2-30-0. On the other hand, the stiffness of beam BIII-3-30-0 showed fair decrease by about 9% compared to that of BII-2-30-0.

Using internal fibers resulted in increase the ultimate capacity as well decrease the exhibited mid-span deflection as depicted in Fig. 12(a). In addition, both the average stiffness and the strain energy for all beams provided by internal short fibers showed significant increases compared to those of control beam made of the RCA having the same replacement ratio without internal fibers. The percentages of increases in the strain energies of beams BIV-2-30-1, BIV-2-30-1.5 and BIV-2-30-2 were about 67%, 27% and 56%, respectively, while the percentages of increases in the average secant stiffness were about 31%, 90% and 100%, respectively, for beams BIV-2-30-1, BIV-2-30-1.5 and BIV-2-30-2 compared to those of beam BII-2-30-0.

Regarding the curing method of the recycled coarse aggregate, it could be concluded that the beams cured with cement slurry technique showed more enhanced effect on the secant stiffness and the mid-span deflection than those exhibited by the beam cured by compound SBR method as depicted in Fig. 12(b). The percentages of increases in the secant stiffness were about 24% and 8%, respectively for beams BV-2-30-0-C1 and BV-2-30-0-C2 compared to that of beam BII-2-30-0. Combined the effect of cement slurry curing and the internal short fiber enabled the beam BV-2-30-1.5-C1 to show outstanding performance in both the secant stiffness and the developed strain energy. The percentages of increases in the secant stiffness and the strain energy were about 33% and 38%, respectively for beam BV-3-30-1.5-C1 compared to those of control beam BI-2-0-0 without any recycled coarse aggregate.

3.5. Developed strain

Table 8 summarizes the recorded normal strains developed on the main tensile steel bars as well as the calculated shear strains on the concrete surface based on Eq. (1) [23]. Based on the material properties of the used steel bars, the yield strain is 2100 micro-strain. It can be noticed that the main tensile steel of all beams did not develop the yielding strain. It could be attributed to that the provided cross-sectional area of the main tensile steel was chosen in order to enable the beams to sustain flexural failure load higher than that required to trigger the shear failure of the beams.

Table 8 indicates that the developed tensile strain on the main tension steel decreased as the recycled aggregate replacement ratio increased. Whereas, the tensile strain decreased as shear span-to-depth ratio decreased as illustrated in Table 8. Providing polypropylene discrete fibers led to decrease the tensile strain. That is because the concrete contributed in the tensile resistance owing to the bridging effect of the internal fibers. Curing the recycled coarse aggregate resulted in enhanced the concrete tensile strength leading to decrease the developed tensile strain on the main tensile steel.

As for the developed shear strain on the concrete surface at the unreinforced side, Figs. 13 and 14 show the relationship between the developed shear stress and the calculated shear strain for all beams of groups G2, G3, G4 and G5. It could be noticed that the shear strain increased by increasing the recycled aggregate replacement ratio and increased as the shear span-to- depth ratio

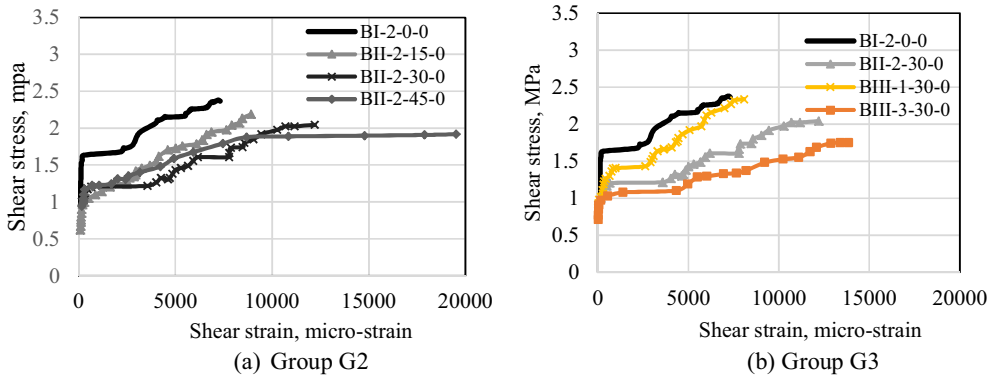


Fig. 13. Shear stress versus shear strain for all specimens of groups G2 and G3.

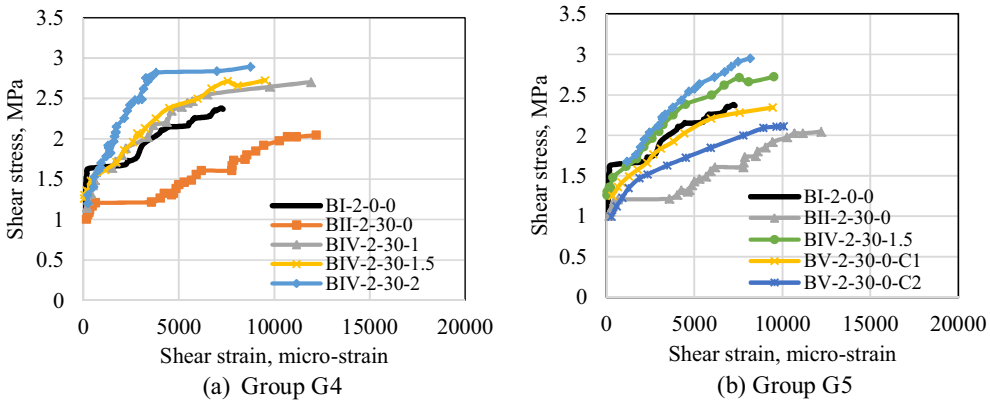


Fig. 14. Shear stress versus shear strain for all specimens of groups G4 and G5.

increased. In addition, the shear strain decreased as the fiber volumetric ratio increased compared to that of beam BII-2-30-0 owing to the enhanced shear behavior of fibrous concrete. Furthermore, the developed shear strain for cured beams with cement slurry and compound SBR curing methods decreased by about 23% and 17%, respectively, compared to that of beam BII-2-30-0. The developed shear strain for beam BV-2-30-1.5-C1 decreased by about 14% compared to that of beam BIV-2-30-1.5. This could be attributed to that the curing method enhanced the bond strength between the cured coarse aggregate, which resulted in decrease the developed shear strain.

4. Analytical study on the shear behavior of RC beams made of recycled coarse aggregate

The current analytical study on the shear behavior of RC beams made of recycled coarse aggregate had been divided into three main stages. In the first stage, the resisting shear forces for the tested beams had been compared against those recommended by different international codes. Then, an equation was proposed in order to calculate the shear force for RC beams made of RCA taking into account different parameters such as the RCA replacement ratio, the shear span-to-depth ratio and the volumetric ratio of the provided internal short fibers. Finally, the proposed equation was verified against the current experimental test results as well as the experimental results of other researchers.

4.1. Comparison between the experimental test results and those stipulated by selected international design codes

In this stage, the experimental shear forces for the tested beams are compared against the calculated shear forces according to the American Concrete Institute Code (ACI 318-14) [33], Canadian Standard Association Code (CSA 23.3 2004) [34], European Code (EC2-04) [35] and the Egyptian Code of Practice ECP 203-17) [36].

According to the ACI318-14 code, the shear force, V_{pre}, can be calculated by Eq. (2).

$$V_{pre} = \left[0.16\lambda\sqrt{f'_c} + 17\rho_w\left(\frac{V_u.d}{M_u}\right)\right]b_w.d \quad (2)$$

where λ is a concrete parameter equal to 1.00 for the normal weight concrete; f'_c is concrete compressive cylinder strength; ρ_w is longitudinal reinforcement ratio, V_u is factored shear force at the considered section and M_u is the corresponding factored moment at that section.

The predicted shear force, V_{pre}, based on Canadian provisions (CSA 23.3-2004) is calculated by Eq. (3).

$$V_{pre} = \lambda\beta\sqrt{f'_c}.b_w.d \quad (3)$$

Where λ is the strength reduction factor equal to 1.00 for the normal density concrete; β is the factor for accounting for the shear resistance of cracked concrete = $\frac{230}{1000+d_v}$ when the section contains no transverse reinforcement and a_g >20 mm, $\frac{230}{1000+s_{ze}}$ when the section contains no transverse reinforcement and a_g ≤20 mm.

According to the European code (EC2-04), the shear force, V_{pre}, is calculated by Eq. (4).

$$V_{pre} = [C_{Rd,c}.k(100\rho_1 f_{ck})^{1/3}]b_w.d \quad (4)$$

where $C_{Rd,c} = 0.18$, $k = 1 + \sqrt{\frac{200}{d}}$, ρ_1 is the longitudinal reinforcement ratio and f_{ck} is the characteristic compressive cylinder strength of concrete at 28 days.

The predicting shear force, V_{pre}, based on the Egyptian code of practice (ECP 203-17) is calculated by Eq. (5).

$$V = 0.24\sqrt{f_{cu}}b_w d \quad (5)$$

where f_{cu} is concrete compressive cube strength.

Table 9 summarizes the recorded concrete shear strength of all specimens along with the calculated values according to the adopted design standard taking into account the relevant material properties. It is worth mentioning that the used values for the experimental concrete shear strengths for each beam were chosen to be the corresponding shear forces to the first shear cracking loads as listed in Table 8. In addition, the calculated shear resistances based on the design standard provisions are for normal strength concrete without recycled coarse aggregate. Therefore, the comparison is correct for only the beam BI-2-0-0 without recycled coarse aggregate. However, the comparison was undertaken for all specimens. That is to show the accuracy of the codes' equations when applied on RC beams made of both crude and cured RCA and provided by internal Polypropylene short fibers.

Based on the results summarized in Table 9, it could be noticed that the result of the CSA code is the most conservative one, while the result of the ECP is the least conservative one. That is for the control beam BI-2-0-0 without recycled coarse aggregate. However, the same trend was observed for the other beams made of recycled coarse aggregate inspite that the experimental shear resistances were changed according to the recycled aggregate replacement ratio, the shear span-to-depth ratio, the fiber volumetric ratio and the curing method. Although, the results of the

Table 9
Experimental results versus codes' predictions (VExp./Vpre) for all test beams.

Group No.	Specimen	f_c MPa	V_{Exp} kN (4)	V_{pre} ACI (5)	V_{pre} CSA (6)	V_{pre} EC (7)	V_{pre} ECP (8)	(4)/(5)	(4)/(6)	(4)/(7)	(4)/(8)
G1	BI-2-0-0	23.04	60.00	35.62	33.12	46.78	48.29	1.68	1.81	1.28	1.24
G2	BII-2-15-0	22.56	55.50	35.32	32.77	46.45	47.79	1.57	1.69	1.19	1.16
	BII-2-30-0	21.52	36.50	34.65	32.00	45.73	46.67	1.05	1.14	0.80	0.78
	BII-2-45-0	20.00	35.50	33.65	30.86	44.62	45.00	1.05	1.15	0.80	0.79
G3	BIII-1-30-0	21.44	41.50	41.42	31.95	45.67	46.59	1.00	1.30	0.91	0.89
	BIII-3-30-0	21.20	29.00	32.17	31.76	45.50	46.33	0.90	0.91	0.64	0.63
G4	BIV-2-30-1	22.65	47.50	35.37	32.77	46.45	47.79	1.34	1.45	1.02	0.99
	BIV-2-30-1.5	23.44	49.00	35.87	33.41	47.05	48.72	1.37	1.47	1.04	1.01
	BIV-2-30-2	25.52	52.00	37.13	34.85	48.40	50.82	1.40	1.49	1.07	1.02
G5	BV-2-30-0-C1	23.80	43.00	36.09	33.66	47.29	49.08	1.19	1.28	0.91	0.88
	BV-2-30-0-C2	22.00	37.00	34.96	32.36	46.17	47.19	1.06	1.14	0.80	0.78
	BV-2-30-1.5-C1	24.72	62.50	36.65	34.31	47.89	50.03	1.71	1.82	1.31	1.25
Average								1.28	1.39	0.98	0.95
Standard deviation								0.28	0.29	0.21	0.20
Coefficient of variation (COV)								4.64	4.84	4.67	4.84

V_{Exp} = Experimental first shear cracking load; V_{pre} = Predicted shear force according to relevant code; ACI = ACI-318-14; CSA = CSA 23.3-2004; EC = EC2-04; ECP = ECP 203-2017. b = 150 mm, d = 250 mm, ρ_w% = 2.144%

CSA code are the most conservative results, while the results of the ECP are the least conservative ones. Furthermore, for some beams, due to the increase in the recycled coarse aggregate replacement ratio (30% and 45%) and the change of the shear span-to-depth ratio, the shear resistance of the relevant beams showed significant decrease below the stipulate limits set by design standards. That happened for specimens BII-2-30-0, BII-2-45-0, BIII-1-30-0, BIII-3-30-0, BV-2-30-0-C1 and BV-2-30-0-C2. This means that the codes' equations cannot reasonably apply to calculate the shear resistance of RC beams made of RCA. Thus, correction factors have to be used to consider the effects of RCA replacement ratio, the shear span-to-depth ratio and the volumetric ratio of the provided internal short fibers.

4.2. Proposed equation for the shear capacity for RC beams made of RCA

In the current study, the studied four key parameters are the recycled coarse aggregate replacement ratio (RCA%), the shear span-to-depth ratio (a/d), the fiber volumetric ratio (V_f %) and the curing methods by cement slurry and Compound SBR. Therefore, in order to investigate the effect of each parameter on the shear capacity of RC beams made of RCA, the experimental shear capacities were first normalized by dividing them by $bd\sqrt{f_c}$ and then the effect of the first three parameters on the shear capacity was highlighted taking into account the relevant material properties as summarized in Table 10. Accordingly, three factors are assumed; namely, k_1, $k_2$and $k_3$in order to take into account the effects of RCA%, a/d and the fiber volumetric ratio V_f % on the shear capacity of RC beams.

Table 10
Normalized shear capacity for all test beams.

Beam ID	f'_c (MPa)	P_u, kN	V_{exp}, kN	$V_{exp}/bd\sqrt{f'_c}$
BI-2-0-0	23.04	178	89.0	0.49
BII-2-15-0	22.56	164	82.0	0.46
BII-2-30-0	21.52	153	76.5	0.44
BII-2-45-0	20.00	144	72.0	0.43
BIII-1-30-0	21.44	175	87.5	0.50
BIII-3-30-0	21.20	113	56.5	0.33
BIV-2-30-1	22.56	202	101.0	0.56
BIV-2-30-1.5	23.44	205	102.5	0.56
BIV-2-30-2	25.52	217	108.5	0.57
BV-2-30-0-C1	23.80	176	88.0	0.48
BV-2-30-0-C2	19.84	158	79.0	0.45
BV-2-30-1.5-C1	24.72	221	110.5	0.59

4.2.1. Effect of recycled coarse aggregate replacement ratio (RCA%)

To find out the effect of RCA% on the shear capacity, a relationship between the normalized shear capacities and the recycled aggregate replacement ratio RCA% is constructed as depicted in Fig. 15. Thus, the trend line for such relationship can be used to demonstrate the effect of the recycled coarse aggregate replacement ratio through the Eq. (6) as given by factor k_1

$$k_1 = 1 + 0.003(RCA\%) \quad (6)$$

It is worth mentioning that the normalization on the shear capacities was considered by dividing the shear capacities of all beams by the shear capacity of control beam, BI-2-0-0, without recycled coarse aggregate.

4.2.2. Effect of shear span-to-depth ratio (a/d)

In order to consider the effect of the shear span-to-depth (a/d) ratio on the shear capacity of RC beams made of recycled coarse aggregate, a relationship between the normalized shear capacities and the shear span-to-depth ratio is constructed as depicted in Fig. 16. Thus, the trend line for such relationship can be used to demonstrate the effect of the shear span-to-depth ratio through Eq. (7) as given by factor k_2.

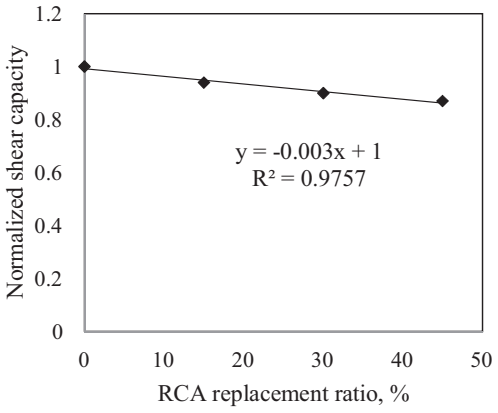


Fig. 15. Normalized shear capacity versus RCA%.

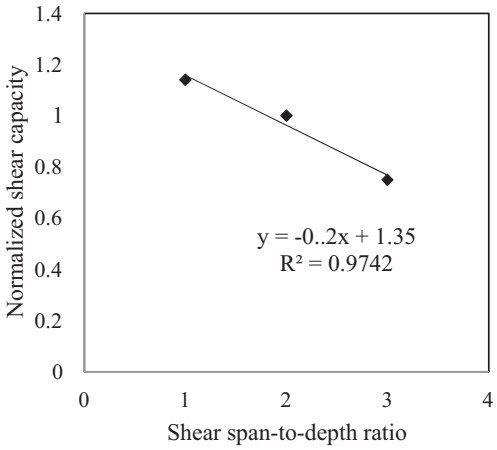


Fig. 16. Normalized shear capacity versus a/d ratio.

$$k_2 = 1.35 - 0.2\left(\frac{a}{d}\right) \quad (7)$$

It is worth mentioning that the normalization on the shear capacities was considered by dividing the shear capacities of the considered beams by the shear capacity of the beam, BII-2–30-0, which has 30% replacement ratio in order to eliminate such effect.

4.2.3. Effect of fiber volumetric ratio

In the same way, the effect of the fiber volumetric ratio on the shear capacity of RC beams made of recycled coarse aggregate can be taken into account through factor k_3 that expressed in Eq. (8), which obtained from the relationship depicted in Fig. 17.

$$k_3 = 1 + 0.32(V_f) - 0.09\left(V_f^2\right) \quad (8)$$

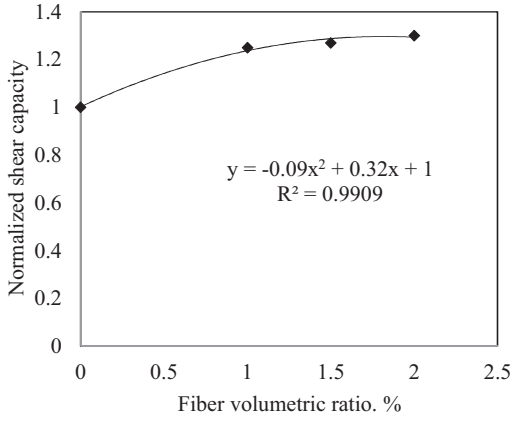


Fig. 17. Normalized shear capacity versus fiber volumetric ratio.

Thus the shear capacity of RC beams made of recycled coarse aggregate can be calculated from the proposed equation (Eq. (9)) that takes into account the effects of recycled aggregare raplacment ratio, shear span-to-depth ratio and the fiber voulmetric ratio.

$$V_{proposed} = 0.45.k_1.k_2.k_3\sqrt{f'_c}b_w d \quad (9)$$

4.3. Verification of the proposed equation agianst experimental results

In order to verify the accuracy of the proposed equation for the shear capacity, the experimental shear resistances for all tested beams are compared with those obtained from the application of the proposed equation taking into account different parameters along with the relevant concrete strength of each beam. Table 11 shows comparison between the experimental shear forces and the calculated shear forces based on the proposed equation for all beams. It can be observed that the proposed equation gives conservative shear force considering all test parameters. In addition, the variation in the results of the proposed equation is between 2.4% and 15.9 with an average variation of about 8.5%, while the coefficient of variation is about 4.6%. That means the results of the proposed equation showed good agreement with the experiment results with an average variation of about 8.5%. It was expected to obtained good results for the proposed equation when its results were compared with the experimental results. Thus, in order to generalize the applicability of the proposed equation, experimental results for 80 beams tested by various researchers have been selected and verified [14–16,19,21,25–27] against the results of the proposed equation. The shear capacities of all considered 80 beams have been calculated based on the proposed equation taking into account the relevant material properties (Refer to Table 12) and then compared with their experimental capacities.

Fig. 18 shows the relationship between the predicted shear capacities and the experimental results for 80 RC beams. It can be observed that the proposed equation gives good results compared with the experimental results of other researchers with an average variation of about 8.3%. However, some scattered results of Choi et al. [21], Fathifazl et al. [27] and Kathuda and Shatarat [26] resulted in increased the coefficient of variation to about 21.9%. It could be concluded that the proposed equation showed satisfactory results compared with the experimental results of the current study as well as those conducted by other researchers.

Table 11
Validation of the proposed equation against the experimental results.

Beam ID	f'_c (MPa)	P_u, kN	Vexp, kN	k1	k2	k3	Vpro, kN	Vpro/Vexp
BI-2-0-0	23.04	178	89.0	1	0.95	1	80.03	0.899
BII-2-15-0	22.56	164	82.0	0.955	0.95	1	75.63	0.922
BII-2-30-0	21.52	153	76.5	0.91	0.95	1	70.38	0.920
BII-2-45-0	20.00	144	72.0	0.865	0.95	1	64.50	0.896
BIII-1-30-0	21.44	175	87.5	0.91	1.15	1	85.04	0.972
BIII-3-30-0	21.20	113	56.5	0.91	0.75	1	55.15	0.976
BIV-2-30-1	22.56	202	101.0	0.91	0.95	1.26	90.80	0.899
BIV-2-30-1.5	23.44	205	102.5	0.91	0.95	1.32	97.14	0.948
BIV-2-30-2	25.52	217	108.5	0.91	0.95	1.34	102.70	0.947
BV-2-30-0-C1	23.80	176	88.0	0.91	0.95	1	74.02	0.841
BV-2-30-0-C2	19.84	158	79.0	0.91	0.95	1	67.58	0.855
BV-2-30-1.5-C1	24.72	221	110.5	0.91	0.95	1.32	99.76	0.903
Average								0.915
Standard deviation								0.042
Coefficient of variation (COV)								0.046

Table 12
Experimental shear capacities of other researchers versus the proposed shear capacities based on the proposed equation.

Research	f'_c	Vexp	Test parameters			*k1*	*k2*	*k3*	b	d	Vpro	Vpro/Vexp
			RCA%	a/d	fiber%							
Fonteboa and Adella [19]	40.5	90.64	0	3.3	0	1	0.69	1	200	264	96.34	1.063
	39.65	88.86	50	3.3	0	0.85	0.69	1	200	264	81.11	0.913
Etxeberria et al. (2007) [15]	41.91	100.50	0	3.3	0	1	0.69	1	200	310	114.88	1.143
	42.38	104.00	25	3.3	0	0.925	0.69	1	200	310	106.80	1.027
	41.34	89.00	50	3.3	0	0.85	0.69	1	200	310	97.05	1.090
	39.75	84.00	100	3.3	0	0.7	0.69	1	200	310	78.53	0.935
Choi et al. (2010) [21]	24.66	176.35	0	1.5	0	1	1.05	1	200	400	177.68	1.008
	24.66	90.70	0	2.5	0	1	0.85	1	200	400	143.84	1.586
	24.56	161.70	30	1.5	0	0.91	1.05	1	200	400	161.40	0.998
	24.56	80.85	30	3.25	0	0.91	0.7	1	200	400	107.60	1.331
	24.15	152.88	50	1.5	0	0.85	1.05	1	200	400	149.62	0.979
	24.15	71.54	50	3.25	0	0.85	0.7	1	200	400	99.74	1.394
	22.56	107.80	100	1.5	0	0.7	1.05	1	200	400	119.50	1.108
	22.56	84.77	100	2.5	0	0.7	0.85	1	200	400	96.73	1.141
	22.56	57.77	100	3.25	0	0.7	0.7	1	200	400	79.66	1.379
	24.15	87.71	50	2.5	0	0.85	0.85	1	200	400	121.12	1.381
	22.56	70.07	100	2.5	0	0.7	0.85	1	200	400	96.73	1.381
	22.56	84.77	100	2.5	0	0.7	0.85	1	200	400	96.73	1.141
Asamoah et al. (2009) [25]	19.8	38.53	0	2.9	0	1	0.77	1	140	230	47.51	1.233
	19.8	46.23	0	2.9	0	1	0.77	1	140	230	47.51	1.028
	19.8	56.49	0	2.9	0	1	0.77	1	140	230	47.51	0.841
	19.8	70.18	0	2.9	0	1	0.77	1	140	230	47.51	0.677
	19.8	87.30	0	2.9	0	1	0.77	1	140	230	47.51	0.544
	14.6	29.08	50	2.9	0	0.85	0.77	1	140	230	35.21	1.211
	14.6	36.78	50	2.9	0	0.85	0.77	1	140	230	35.21	0.957
	8.5	35.97	50	2.9	0	0.85	0.77	1	140	230	27.60	0.767
	8.5	49.66	50	2.9	0	0.85	0.77	1	140	230	27.60	0.556
Fathifazl et al. (2011) [27]	43.5	195.00	74.3	1.5	0	0.777	1.05	1	200	300	133.69	0.686
	43.5	106.00	74.3	4	0	0.777	0.55	1	200	309	72.13	0.680
	36.9	103.00	63.5	2.7	0	0.81	0.81	1	200	309	102.76	0.998
	36.9	83.00	63.5	4	0	0.81	0.55	1	200	305	68.87	0.830
Li et al. (2013) [16]	39.6	97.84	100	1.5	0	0.7	1.05	1	151	364	105.75	1.081
	39.6	98.85	100	1.5	0	0.7	1.05	1	153	365	107.45	1.087
	39.6	89.30	100	2	0	0.7	0.95	1	154	367	98.39	1.102
	39.6	87.48	100	2	0	0.7	0.95	1	151	369	97.00	1.109
	40.8	75.48	100	3	0	0.7	0.75	1	150	362	75.64	1.002
	40.8	76.85	100	3	0	0.7	0.75	1	153	364	77.57	1.009
	40.8	100.42	100	1.5	0	0.7	1.05	1	152	365	108.19	1.077
	40.8	99.92	100	1.5	0	0.7	1.05	1	150	366	107.06	1.071
	38.88	102.18	100	1.5	0	0.7	1.05	1	154	367	107.85	1.055
	38.88	102.68	100	1.5	0	0.7	1.05	1	155	367	108.55	1.057
	38.88	104.19	100	1.5	0	0.7	1.05	1	152	365	105.87	1.016
	38.88	102.89	100	1.5	0	0.7	1.05	1	151	364	104.88	1.019
	39.28	87.27	100	2	0	0.7	0.95	1	153	364	96.60	1.107
	39.28	87.49	100	2	0	0.7	0.95	1	154	363	96.96	1.108
	39.28	70.89	100	3	0	0.7	0.75	1	150	363	74.56	1.052
	39.28	71.89	100	3	0	0.7	0.75	1	153	362	75.84	1.055
Knaack and Kurama (2014) [14]	31.2	36.90	0	3.8	0	1	0.59	1	150	200	41.62	1.128
	46.4	42.30	0	3.8	0	1	0.59	1	150	200	49.76	1.176
	41.8	44.00	50	3.8	0	0.85	0.59	1	150	200	40.35	0.917
	37.4	43.70	50	3.8	0	0.85	0.59	1	150	200	38.38	0.878
	39.1	38.00	100	3.8	0	0.7	0.59	1	150	200	32.25	0.849
	39.2	39.90	100	3.8	0	0.7	0.59	1	150	200	32.29	0.809
	24.66	158.40	0	1.5	0	1	1.05	1	200	360	159.91	1.010
	24.56	145.40	30	1.5	0	0.91	1.05	1	200	360	145.26	0.999
	24.15	137.52	50	1.5	0	0.85	1.05	1	200	360	134.66	0.979
	22.56	97.20	100	1.5	0	0.7	1.05	1	200	360	107.55	1.106
	24.56	73.40	30	2.5	0	0.91	0.85	1	200	360	117.59	1.602
	24.15	79.20	50	2.5	0	0.85	0.85	1	200	360	109.01	1.376
	22.56	76.32	100	2.5	0	0.7	0.85	1	200	360	87.06	1.141
	24.56	73.70	30	3.5	0	0.91	0.65	1	200	360	89.92	1.220
	24.15	64.08	50	3.5	0	0.85	0.65	1	200	360	83.36	1.301
	22.56	51.84	100	3.5	0	0.7	0.65	1	200	360	66.58	1.284
Kathuda and Shatarat (2016) [26]	28.3	69.30	0	2	0	1	0.95	1	206	250	110.10	1.589
	25.2	58.94	50	2	0	0.85	0.95	1	206	250	88.83	1.507
	23.2	55.04	100	2	0	0.7	0.95	1	206	250	70.48	1.281
	28.05	72.98	50	2	0	0.85	0.95	1	206	250	93.22	1.277
	26.6	66.79	100	2	0	0.7	0.95	1	206	250	74.95	1.122
	28.3	52.51	0	3	0	1	0.75	1	206	250	86.92	1.655
	25.2	49.07	50	3	0	0.85	0.75	1	206	250	70.13	1.429
	23.2	46.45	100	3	0	0.7	0.75	1	206	250	55.64	1.198
	28.05	55.06	50	3	0	0.85	0.75	1	206	250	73.59	1.337
	26.6	55.61	100	3	0	0.7	0.75	1	206	250	59.17	1.064

Table 12 (*continued*)

Research	f'_c	Vexp	Test parameters			*k1*	*k2*	*k3*	b	d	Vpro	Vpro/Vexp
			RCA%	a/d	fiber%							
	41.6	186.00	63.5	1.5	0	0.81	1.05	1	200	300	136.50	0.734
	41.6	168.00	63.5	2	0	0.81	0.95	1	200	300	123.50	0.735
	41.6	105.00	63.5	2.59	0	0.81	0.832	1	200	309	111.40	1.061
	37.1	92.70	0	2.59	0	1	0.832	1	200	309	130.71	1.410
	41.6	85.40	63.5	3.93	0	0.81	0.564	1	200	305	74.54	0.873
	34.4	148.32	0	2.59	0	1	0.832	1	200	309	126.34	0.852
	49.1	103.70	74.3	3.93	0	0.777	0.564	1	200	305	77.10	0.743
	Average											1.083
	Standard deviation											0.237
	Coefficient of variation (COV)											0.219

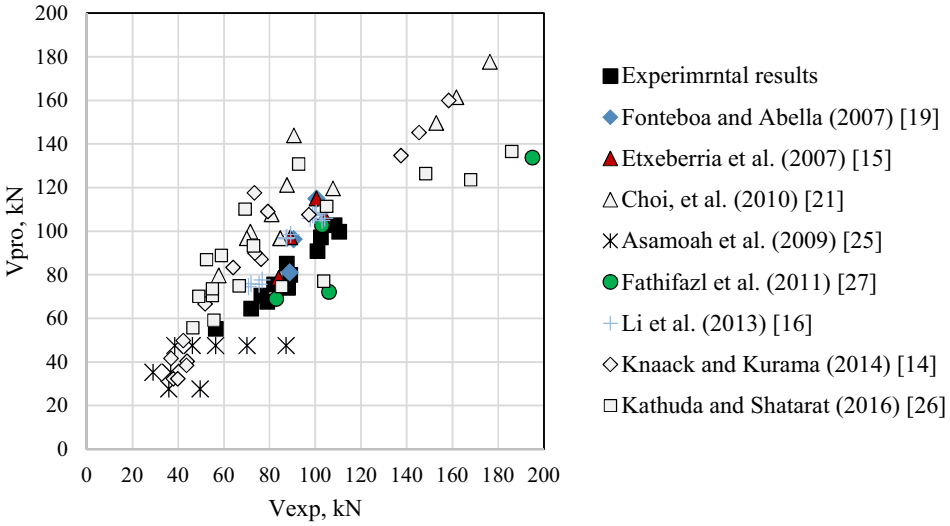


Fig. 18. Proposed shear forces (Vpro) versus experimental shear forces (Vexp).

5. Conclusion

In the current study, the effects of recycled coarse aggregate replacement ratio (RCA %), shear span- to-depth ratio (a/d), fiber volumetric ratio, and surface curing methods on the shear performance of RC beams made of recycled aggregate have been investigated. Based on the concrete dimensions as well as the reinforcement detailing of the tested beams, the following conclusions are drawn:

1. Partial replacement of the recycled coarse aggregate showed insignificant effect on the crack pattern and failure mode of reinforced concrete beams made of recycled coarse aggregate. In contrary, it showed significant effect on the ultimate shear capacity. The percentages of decreases in the shear capacities were about 8%, 14% and 19%, respectively, for RC beams provided by RCA replaced by 15%, 30% and 45%. Besides, the major crack width of recycled aggregate concrete beams becomes wider than that of the control beam owing to the weak bonding between the old cement paste covering the recycled aggregate and new mixture.
2. Increasing the replacement ratio of the recycled coarse aggregate resulted in accelerating the appearance of both flexural and shear cracks compared to those of control virgin beam without any recycled aggregate. That is due to the presence of minute pores in the adhered mortar to the RCA along with the developed continuous cracks and fissures inside the RCA due to the crushing process. Such effects resulted in increasing the weakness of the concrete as the RCA replacement ratio increased
3. Increasing the volumetric ratio of the added short fibers resulted in hindering the appearance of both flexural and shear cracks compared to that of the control beam made of recycled coarse aggregate without any fibers.
4. Increasing the replacement ratio of the recycled coarse aggregate results in decrease the shear strength proportionally. However, the decreases in the shear strength could be compensated by providing internal short fibers. Accordingly, increasing the volumetric ratio of the internal fibers resulted in increase the shear strength compared with those of RC beam made of recycled aggregate without internal fibers. Providing internal short fibers by volumetric ratios of 1%, 1.5% and 2% enabled the RC beams made of 30% partial replacement of the recycled coarse aggregate to compensate the decreases in the shear capacities (14%) and to increase their shear capacities by about 13%, 15% and 22% compared to those of the control beam, respectively.
5. Increasing the replacement ratio of the recycled aggregate resulted in decreasing the shear stiffness proportionally, where the shear strain increases significantly with increasing the replacement ratio of the recycled aggregate at the same shear stress level. On contrary, for the recycled aggregate beam, increasing the fiber volumetric ratio resulted in decreasing the shear strain at the same shear stress level.
6. Curing the recycled coarse aggregate using cement slurry showed significant enhancement on the shear strength of RC beam made of cured recycled aggregate, which exceeded the corresponding shear strength of control beam with recycled coarse aggregate. On contrary, curing the recycled coarse aggregate by compound SBR showed lower enhancement compared

to that of the other curing technique. Thus, the restored shear capacities were about 15% and 3% for beams provided by cured coarse aggregate based on cement slurry and compound SBR, respectively compared to that of the beam made of crude RCA.

7. The proposed equation showed satisfactory results compared with the experimental results of the current study with no more than 8.5% variation as well as with those conducted by other researchers with no more than 22% variation.

Conflicts of interest

None.

References

[1] M. Fardis, Innovation Materials and Techniques in Concrete Construction, Department of Civil Engineering, University of Patras, Greece, 2012.
[2] M. Pepe, A Conceptual Model for Designing recycled Aggregate Concrete for Structural Application (Doctoral Thesis), University of Salerno, Italy, 2015.
[3] C. Kou, S. Poon, D. Chan, Properties of steam cured recycled aggregate fly ash concrete. International RILEM Conference on The Use of Recycled Materials in Building and Structures, Barcelona, 2004: 590–559
[4] A. Katz, Treatment for the improvement of recycled aggregate, J. Mater. Civil Eng. 16 (2004) 597–603.
[5] S. Ismail, M. Ramli, Influence of surface treated coarse recycled concrete aggregate on compressive strength of concrete, Int. J. Civil, Environ., Struct., Constr. Arch. Eng. 8 (8) (2014) 881–885.
[6] K. Abhiram, P. Saravanakumar, Properties of recycled aggregate concrete containing hydrochloric acid treated recycled aggregates, Inter. J. ChemTech Res. 8 (1) (2015) 72–78.
[7] V. Tam, C. Tam, K. Le, Removal of cement mortar remains from recycled aggregate using pre-soaking approaches, Resour. Conserv. Recycl. 50 (2006) 82–101.
[8] J. Li, H. Xiao, Y. Zhou, Influence of coating recycled aggregate surface with pozzolanic powder on properties of recycled aggregate concrete, Constr. Build. Mater. 23 (2009) 1287–1291.
[9] S. Kou, C. Poon, Properties of concrete prepared with PVA- impregnated recycled concrete aggregates, Cem. Concr. Compos. 32 (2010) 649–654.
[10] J. Sagaseta, R. Vollum, Influence of aggregate fracture on shear transfer through cracks in reinforced concrete, Mag. Concr. Res. 63 (2011) 119–137.
[11] S. Sadati, M. Arezoumandi, K. Khayat, J. Volz, Shear performance of reinforced concrete beams incorporating recycled concrete aggregate and high-volume fly ash, J. Cleaner Prod. 115 (2016) 284–293.
[12] H. Yun, Y. You, D. Lee, Effects of replacement ratio of recycled coarse aggregate on the shear performance of reinforced concrete beams without shear reinforcement, LHI J. 2 (2011) 471–477.
[13] S. Kim, C. Jeong, J. Lee, K. Kim, Size effect in shear failure of reinforced concrete beams with recycled aggregate, J. Asian Arch. Build. Eng. (2013) 323–330.
[14] A. Knaack, Y. Kurama, Behavior of reinforced concrete beams with recycled concrete coarse aggregates, J. Struct. Eng. 12 (2014) 401–409.
[15] M. Etxeberria, E. Vazquez, A. Mari, M. Barra, Influence of amount of recycled coarse aggregates and production process on properties of recycled aggregate concrete, J. Cem. Concr. Res. 37 (2007) 735–742.
[16] C. Li, G. Li, W. Shao, Q. Guo, R. Liu, Shear-crack behaviors of reinforced full-recycled aggregate concrete beams, Appl. Mech. Mater. 438–439 (2013) 794–799.
[17] S. Aly, M. Ibrahim, M. Khattab, Shear behavior of reinforced concrete beams casted with recycled coarse aggregate, Eur. J. Adv. Eng. Technol. 2 (2015) 59–71.
[18] F. Al-Zahraa, M. El-Mihilmy, T. Bahaa, Experimental investigation of shear strength of concrete beams with recycled concrete aggregates, Int. J. Materials and Structural Integrity 5 (2011) 291–310.
[19] B. Fonteboa, F. Abella, Shear strength of recycled concrete beams, Constr. Build. Mater. 21 (2007) 887–893.
[20] P. Khergamwala, J. Singh, R. Kumar, Experimental study on shear behavior of reinforced recycled aggregate concrete beams, Int. J. Civil Eng. Technol. 7 (2016) 128–139.
[21] H. Choi, C. Yi, H. Cho, K. Kang, Experimental study on the shear strength of recycled aggregate concrete beams, Mag. Concr. Res. 62 (2010) 103–114.
[22] O. Lian, L. Wee, M. Masrom, G. Hua, Experimental study on shear behaviour of high strength reinforced recycled concrete beam, Sci. Technol. 2 (2013) 601–610.
[23] M.N. Khaja, E.G. Sherwood, Does the shear strength of reinforced concrete beams and slabs depend upon the flexural reinforcement ratio or the reinforcement strain, Can. J. Civ. Eng. 40 (2013) 1068–1081.
[24] R. Singh, N. Bansal, K. Bedi, Shear behavior of recycled beams, Int. J. Sci. Eng. Res. 6 (2015) 879–888.
[25] M. Asamoah, J. Ampofo, R. Afrifa, Flexural and shear behaviour of reinforced concrete beams made from recycled Materials, J. Ghana Inst. Eng. 6 (2009) 57–66.
[26] H. Katkhuda, N. Shatarat, Shear behavior of reinforced concrete beams using treated recycled concrete aggregate, Constr. Build. Mater. 125 (2016) 63–71.
[27] G. Fathifazl, A. Razaqpur, O. Isgor, A. Abbas, B. Fournier, S. Foo, Shear capacity evaluation of steel reinforced recycled concrete (RRC) beams, Eng. Struct. 33 (2011) 1025–1033.
[28] BS8500-1:2006. Concrete-Complementrary British Standard to BS EN 206-1-Part-2 Specifications for constituent materials and concrete: BSI, 389 Chiswich High Road London.
[29] European Standard EN 14889-2: 2006 fibers for concrete.
[30] V. Kukadia, D. Parekh, R. Gajjar, Influence of aggregate's treatment on properties of recycled aggregate concrete, Int. J. Civil Eng. Technol. 8 (2017) 351–361.
[31] H. Shrinath, B. Kumar, Sumit Avinash, L. Vinodkumar, Influence of treatment method on recycled aggregate concrete made with recycled coarse aggregate, Int. J. Sci. Devel. Res. 1 (2016) 836–842.
[32] G. Awchat, N. Kanhe, Experimental studies on polymer modified steel fibre reinforced recycled aggregate concrete, Int. J. Appl. Innovation Eng. Manage. 2 (2013) 126–134.
[33] A.C.I. Committee, Building Code Requirements for Structural Concrete (ACI 318M–14), American Concrete Institute, Detroit, Mich, 2014.
[34] Canadian Standard, Association CSA23.3, Design of concrete structures, Canadian Standard Assoc. (2004).
[35] EN 1992-1-1, 2004. Eurocode 2: Design of Concrete Structures, Part 1-1, General Rules and Rules for Buildings, European Committee for Standardization, Brussels, Belgium.
[36] Egyptian code for design and construction of reinforced concrete structures (ECP 203–2017), 2017.